Cornous Biology
Research Article

An ultrasound-assisted facile synthesis of pyrazole derivatives; docking, ADMET, FMO analysis and *in vitro* evaluation for anti-microbial activities

Varshitha Mahaveer Jain[1*], Narendra Boraiah Gowda[1*], Bhargav Amaranarayana Reddy[1], Tharun Bharadwaj[2]

[1]Department of Pharmaceutical Chemistry, Visveswarapura Institute of Pharmaceutical Sciences, 22nd Cross, Banashankari 2nd Stage, Bengaluru, Karnataka- 560070, India.
[2]Faculty of Pharmacy, M S Ramaiah University of Applied Sciences, University House, New BEL Road, Mathikere, Bengaluru, Karnataka- 560054, India.

[*]**Correspondence**
Varshitha Mahaveer Jain
varshithajain555@gmail.com
Narendra Boraiah Gowda
nbgowda@gmail.com

Volume: 2, Issue: 3, Pages: 9-22
DOI: https://doi.org/10.37446/corbio/rsa/2.3.2024.9-22
Received: 12 April 2024 / Accepted: 9 August 2024 / Published: 30 September 2024

Background: Green chemistry utilizes methods that are less toxic for the environment by reducing hazardous substance production and improving reaction efficiency. By using ultrasound-catalyzed reactions, it is possible to reduce reaction times drastically and achieve higher yields. Chalcones can be used for synthesizing pyrazoles using this method, as these pyrazoles have good anti-bacterial potential.

Methods: Pyrazole derivatives were synthesized by reacting chalcones with hydrazine hydrate in an ultrasonicator. The compounds were characterized by TLC, melting point, FTIR, and ^{1}H NMR. ADMET studies were performed in software to evaluate drug-likeness. Docking studies were performed in PyRx software, and FMO calculations were done using ORCA software.

Results: Docking studies for antibacterial potential showed compound B5 had the strongest antibacterial binding (-8.8 kcal/mol), which is better than ciprofloxacin (-7.4 kcal/mol). For antifungal, B1 and B8 had higher affinities (-8.7 kcal/mol), compared to fluconazole (-7.5 kcal/mol). Quantum calculations revealed B5 and B9 had the lowest SCF energies, indicating greater stability, while variations in dipole moments suggested differences in polarity affecting solubility and interactions. Compounds B5 and B6 showed consistent antibacterial and antifungal activity across tested strains.

Conclusion: With the growing challenge of anti-bacterial resistance, developing effective and sustainable anti-bacterial agents is crucial. This study efficiently synthesized pyrazole derivatives via ultrasound-assisted green chemistry, showing promising anti-bacterial activity and potential for further optimization.

Keywords: *chalcones, pyrazoles, ultrasonication, molecular docking, anti-bacterial, anti-fungal*

Introduction

Green chemistry, also known as sustainable chemistry, focuses on the design and optimization of processes and products to minimize or eliminate the use of hazardous substances harmful to the environment (Ivanković et al., 2017). Guided by its 12 principles including energy efficiency, incorporation of catalysis, atom economy, and reduction of toxic reagents our research integrates these concepts into the synthesis of bioactive molecules (Anastas et al., 2001). In this context, ultrasound-assisted synthesis has emerged as an attractive approach, as it significantly reduces reaction times and improves yields compared with conventional techniques (Banerjee, 2017). Although ultrasound has been previously employed for the synthesis of pyrazoles, its combination with in-silico and in-vitro evaluations in the present study provides additional mechanistic and biological insights. Chalcones, important intermediates in heterocyclic chemistry, belong to the flavonoid family and represent a diverse class of natural compounds with reported anticancer, anti-bacterial, anti-inflammatory, and antioxidant activities (Rudrapal et al., 2021). Typically synthesized by Claisen–Schmidt condensation (Bukhari et al., 2012), chalcones are versatile precursors for constructing heterocycles such as pyrazoles, pyrimidines, and imidazoles (Teli & Chawla, 2021; Mahmood et al., 2022). Pyrazoles are five-membered heterocycles with two adjacent nitrogen atoms (Jaiswal, 2019). Due to the difficulty in forming N–N bonds naturally, pyrazole scaffolds are relatively rare in nature, yet they have attracted wide attention for their broad pharmacological activities, including antibacterial, antifungal, antiviral, and antioxidant properties (Prasad et al., 2011; Karrouchi et al., 2011; Bécerra, D et al., 2025). In this study, we report the ultrasound-assisted synthesis of pyrazole derivatives from chalcones, coupled with both in-silico and in-vitro evaluations. Beyond demonstrating a green and efficient synthetic route, our work emphasizes the structural features of the synthesized derivatives and correlates them with their antibacterial and antifungal potential, offering insights that extend beyond previously reported ultrasound-based methods.

Materials and methods

Chemistry

All the required chemicals were procured from SPECTROCHEM, CENTRAL DRUG HOUSE (CDH), SIGMA-ALDRICH, SDFCL, and INDIAN CANE POWER LIMITED. The melting points of the synthesized compounds were determined using a MEPA melting point apparatus by LABINDIA. The purity of the compounds was checked by thin layer chromatography (TLC) using Silica gel 60 F_{254} pre-coated plates by Merck with a combination of mobile phase. The spots were visualized under UV light and in an iodine chamber. The IR spectra of the synthesized compounds were recorded using a FT-IR Bruker Alpha 2 at RLJ Pharma Solutions, in the range of 400-4000 cm^{-1}, and the values of V_{max} were reported in cm^{-1}. The ^{1}H-NMR spectra were recorded on a Bruker 400 MHz using $CDCl_3$ as the solvent, and chemical shifts (δ) were reported in parts per million downfield from the internal reference tetramethylsilane (TMS) at the Department of Science and Technology-SAIF, Dharwad, and Chromatogen Analytical Solutions, Mysore.

Step 1: Synthesis of chalcones (A1-A9)

General procedure for synthesis of chalcones (A1-A9)

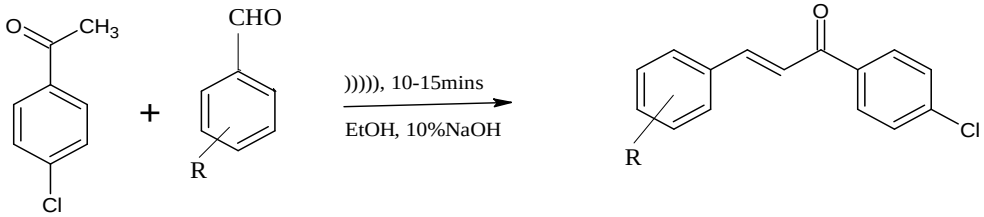

Figure 1. Scheme for the synthesis of chalcones

P-chloroacetophenone (0.01 mol) was dissolved in 15 mL of ethanol in a 250 mL round-bottomed flask, kept for sonication in an ultrasonication bath at the temp. of 35 °C for 15 min, and 4 mL of 10% NaOH was added slowly; immediately the reaction mixture turned a golden yellow color. Then, aromatic aldehyde (0.01 mol) was added through a dropping funnel, and the sonication was continued at room temperature for about 10-15 mins. The precipitate obtained was filtered, washed with water, and recrystallized from ethanol (Figure 1)

(A1) - Chemical name: (2E)-1-(4-chlorophenyl)-3-[4-(propan-2-yl)phenyl]prop-2-en-1-one, Yield: 90%, MP: 82 °C, Rf value (pet ether: ethyl acetate): 0.6, FTIR cm^{-1} : 1660 (C=O), 1594 (C=C), 817 (C-Cl)

(A2) - Chemical name: 1-(4-chlorophenyl)-3-(3-nitrophenyl)prop-2-en-1-one, Yield: 89%, MP: 145 °C, Rf value (pet ether: ethyl acetate): 0.47, FTIR cm^{-1} : 1667 (C=O), 1608 (C=C), 742 (C-Cl)

(A3) - Chemical name: 1-(4-chlorophenyl)-3-(4-methylphenyl)prop-2-en-1-one, Yield: 89%, MP: 122 °C, Rf value (pet ether: ethyl acetate): 0.71, FTIR cm^{-1}: 1653(C=O), 1586 (C=C), 807 (C-Cl)

(A4) - Chemical name: 1-(4-chlorophenyl)-3-(4-nitrophenyl)prop-2-en-1-one, Yield: 90%, MP: 164 °C, Rf value (pet ether: ethyl acetate): 0.66, FTIR cm^{-1}: 1659 (C=O), 1586 (C=C), 754 (C-Cl)

(A5) - Chemical name: 3-(3-chlorophenyl)-1-(4-chlorophenyl)prop-2-en-1-one, Yield: 95%, MP: 104 °C, Rf value (pet ether: ethyl acetate): 0.7, FTIR cm^{-1}: 1659 (C=O), 1603 (C=C), 787 (C-Cl)

(A6) - Chemical name: 1-(4-chlorophenyl)-3-(2,4-dimethoxyphenyl)prop-2-en-1-one, Yield: 84%, MP: 126 °C, Rf value (pet ether: ethyl acetate): 0.55, FTIR cm^{-1}: 1650 (C=O), 1575 (C=C),744 (C-Cl), 1207 (C-O-C)

(A7) - Chemical name: 1-(4-chlorophenyl)-3-(3,4,5-trimethoxyphenyl)prop-2-en-1-one, Yield: 89%, MP: 129 °C, Rf value (pet ether: ethyl acetate): 0.5, FTIR cm^{-1}: 1664 (C=O), 1587 (C=C),781 (C-Cl), 1126 (C-O-C)

(A8) - Chemical name: 1-(4-chlorophenyl)-3-phenylprop-2-en-1-one, Yield: 94%, MP: 100-102 °C, Rf value (pet ether: ethyl acetate): 0.5, FTIR cm^{-1}: 1658 (C=O), 1508 (C=C),761 (C-Cl)

(A9) - Chemical name: 1,3-bis(4-chlorophenyl)prop-2-en-1-one, Yield: 92%, MP: 158 °C, Rf value (pet ether: ethyl acetate): 0.56, FTIR cm^{-1}: 1651 (C=O), 1583 (C=C), 742 (C-Cl).

Step 2: Synthesis of pyrazoles (B1-B9)

General procedure for synthesis of pyrazoles (B).

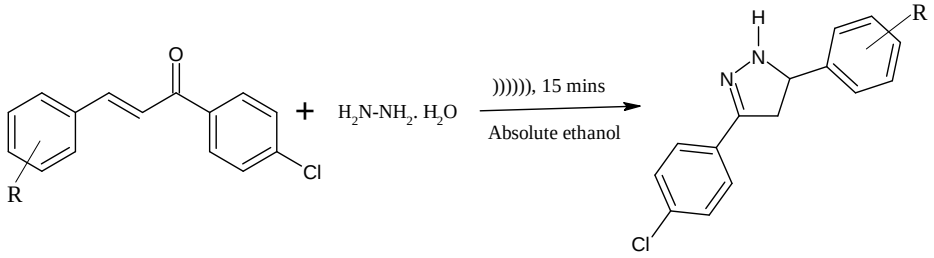

Figure 2. Scheme for the synthesis of pyrazoles from chalcones

Chalcone (0.005 mol) was taken in a 100 mL round-bottom flask, around 8-10 mL of absolute ethanol was added along with hydrazine hydrate (0.025 mol), and the reaction mixture was kept for sonication in an ultrasonication bath at the temp. of 35 °C for 15 min. The reaction mixture is sonicated at room temperature until the reaction is complete. After completion, the reaction mixture was concentrated until crystals appeared and then set aside to allow complete crystal formation. The resulting crystals were filtered, washed with cold aqueous ethanol, and recrystallized from ethanol (Figure 2). Reaction time and the yield of the synthesized compounds are given in Table 1.

(B1) - Chemical name: 3-(4-chlorophenyl)-5-[4-(propan-2-yl)phenyl]-4,5-dihydro-1H-pyrazole Yield: 76%, MP: 179 °C, Rf value (pet ether : ethyl acetate): 0.49, FTIR cm^{-1} : 3215 (N-H), 1566 (C=N), 795 (C-Cl), ^{1}H NMR, $CDCl_3$, 400 MHz : δ 7.633-7.611 (d, 2H, Ar-H), 7.286-7.255 (m, 2H, Ar-H), 7.132-7.112 (d, 2H, Ar-H), 6.992-6.971(d, 2H, Ar-H), 4.949-4.905 (m, 1H, -CH), 4.751-4.707 (m, 1H, -CH), 2.797-2.728 (m, 1H, $-CH_2$), 1.143-1.126 [d, 6H,($-CH_3)_2$]

(B2) - Chemical name: 3-(4-chlorophenyl)-5-(3-nitrophenyl)-4,5-dihydro-1H-pyrazole Yield: 84%, MP: 94.5 °C, Rf value (pet ether : ethyl acetate): 0.36, FTIR cm^{-1} : 3223 (N-H), 1520 (C=N), 734 (C-Cl), ^{1}H NMR, $CDCl_3$, 400 MHz : δ 8.257 (S, 1H, Ar-H), 8.15 (d, 1H, Ar-H), 7.758 (d, 1H, Ar-H), 7.552 (m, 3H, Ar-H), 7.345 (d, 2H, Ar-H), 5.086 (m, 1H, -CH), 3.567 (m, 1H, $-CH_2$), 3.00(m, 1H, $-CH_2$)

(B3) - Chemical name: 3-(4-chlorophenyl)-5-(4-methylphenyl)-4,5-dihydro-1H-pyrazole, Yield: 79%, MP: 104 °C, Rf value (pet ether : ethyl acetate): 0.38, FTIR cm^{-1} : 3110 (N-H), 1505 (C=N), 769 (C-Cl), ^{1}H NMR, $CDCl_3$, 400 MHz : δ 7.958-7.902 (m, 3H, Ar-H), 7.496-7.474 (m, 1H, Ar-H), 7.332-7.312 (m, 1H, Ar-H), 7.311 (m, 2H, -CH),7.286 (m, 2H, $-CH_2$), 7.286 (m, 1H, Ar-H), 6.816 (s, 1H, Ar-H), 2.463-2.346 (m, 3H, $-CH_3$)

(B4) - Chemical name: 3-(4-chlorophenyl)-5-(4-nitrophenyl)-4,5-dihydro-1H-pyrazole, Yield: 82%, MP: 132.5 °C, Rf value (pet ether : ethyl acetate): 0.43, FTIR cm^{-1} : 3349 (N-H), 1510 (C=N), 748 (C-Cl), ^1H NMR, $CDCl_3$, 400 MHz : δ 7.89-7.87 (d, 2H, ArH), 7.26-7.23 (dd, 4H, ArH), 7.03-7.01 (d, 2H), 4.75-4.70 (d, 1H, CH), 3.24-3.17 (dd, 1H, CH), 2.67-2.60 (dd, 1H, CH)

(B5) - Chemical name: 5-(3-chlorophenyl)-3-(4-chlorophenyl)-4,5-dihydro-1H-pyrazole, Yield: 73%, MP: 104 °C, Rf value (pet ether : ethyl acetate): 0.56, FTIR cm^{-1} : 3236 (N-H), 1487 (C=N), 774 (C-Cl), ^1H NMR, $CDCl_3$, 400 MHz : δ 8.299-8.171 (m, 2H, Ar-H), 7.807-7.781 (d, 1H, Ar-H), 7.654-7.553 (m, 3H, Ar-H), 7.387-7.290 (m, 2H, Ar-H), 5.128-5.076 (m, 1H, -CH), 3.610-3.543 (m, 1H, $-CH_2$), 3.043-2.977 (m, 1H, $-CH_2$)

(B6) - Chemical name: 3-(4-chlorophenyl)-5-(2,4-dimethoxyphenyl)-4,5-dihydro-1H-pyrazole, Yield: 74%, MP: 106 °C, Rf value (pet ether : ethyl acetate): 0.25, FTIR cm^{-1} : 3313 (N-H), 1583 (C=N), 781 (C-Cl), ^1H NMR, $CDCl_3$, 400 MHz : δ 7.27-7.28 (d,2H,Ar-H), 7.13 (s,1H,NH), 6.89-6.88 (d,2H,Ar-H), 6.30 (s,1H,Ar-H), 6.12-6.09 (d,2H,Ar-H), 3.51 (s,3H,OCH_3), 3.36 (s,3H,OCH_3), 1.64 (s,2H,CH_2)

(B7) - Chemical name: 3-(4-chlorophenyl)-5-(3,4,5-trimethoxyphenyl)-4,5-dihydro-1H-pyrazole, Yield: 81%, MP: 106 °C, Rf value (pet ether : ethyl acetate): 0.3, FTIR cm^{-1} : 3220 (N-H), 1586 (C=N), 827 (C-Cl), ^1H NMR, $CDCl_3$, 400 MHz : δ 7.126 (d, 1H, Ar-H), 7.306 (d, 1H, Ar-H) 7.467 (d, 1H, Ar-H), 7.21 (m, 2H, Ar-H), 7.121 (d, 2H, Ar-H), 5.592 (m, 1H, -CH), 5.238 (m, 1H, -CH2), 4.032 (S, 3H, OCH_3), 4.022 (S, 3H, OCH_3), 3.671 (S, 3H, OCH_3), 3.215 (m, 1H, $-CH_2$)

(B8) - Chemical name: 3-(4-chlorophenyl)-5-phenyl-4,5-dihydro-1H-pyrazole, Yield: 80%, MP: 211.5 °C, Rf value (pet ether : ethyl acetate): 0.51, FTIR cm^{-1} : 3143 (N-H), 1477 (C=N), 755 (C-Cl), ^1H NMR, $CDCl_3$, 400 MHz : δ 13.42 (s,1H,NH), 7.86-7.2 (m,9H,ArH), 3.36 (s,2H,CH_2), 2.49 (s,1H,CH)

(B9) - Chemical name: 3,5-bis(4-chlorophenyl)-4,5-dihydro-1H-pyrazole, Yield: 79%, MP: 238.5 °C, Rf value (pet ether : ethyl acetate): 0.54, FTIR cm^{-1} : 3137 (N-H), 1489 (C=N), 828 (C-Cl), ^1H NMR, $CDCl_3$, 400 MHz : δ 7.633-7.611 (d, 2H, Ar-H), 7.286-7.255 (m, 2H, Ar-H), 7.132-7.112 (d, 2H, Ar-H), 6.992-6.971 (d, 2H, Ar-H), 4.949-4.905 (m, 1H, -CH), 4.751-4.707 (m, 1H, $-CH_2$), 2.797-2.728 (m, 1H, $-CH_2$).

Table 1. Reaction time and the yield obtained of the compounds

Compound code	**B1**	**B2**	**B3**	**B4**	**B5**	**B6**	**B7**	**B8**	**B9**
Time taken in minutes	16	15	15	15	17	16	16	17	20
Yield in %	76	84	79	82	73	74	81	80	79

In silico studies

Drug-likeness And ADMET Properties

The drug-likeness was studied by calculating lipinski's rule of 5 by analyzing molecular weight, Log P, H-bond acceptors, and H-bond donors in SwissADME, molinspiration, and A (absorption), D (distribution), M (metabolism), E (elimination) and T (toxicity) of the compounds were performed using pKCSM. Both are open-access websites for the prediction of pharmacokinetic properties of the compounds.

Molecular descriptor calculation

Molecular descriptors for the synthesized compounds and standard drugs (ciprofloxacin and fluconazole) were calculated using the ChemDes web server. The following descriptors were selected for their ability to provide a comprehensive understanding of the molecular properties relevant to biological activity. More clearly, they are quantitative parameters of physical, chemical, or topological properties of chemical molecules that summarize our knowledge and understanding of structure and activity from various aspects.

These descriptors were selected to cover various aspects of molecular structure and behavior that are relevant to the biological activities of the synthesized compounds.

Molecular docking studies

The molecular docking study was conducted using PyRx version 0.8 to assess how the ligands bind to bacterial and fungal enzymes. We first reviewed the literature to determine where the ligands might interact with the target proteins. The 3D crystal structures of the target proteins were downloaded from the RCSB Protein Data Bank (DNA gyrase PDB ID: 6KZX, 14α-demethylase PDB ID: 7RTQ) (Sharif et al., 2021; Rathee et al., 2024) and prepared using Biovia Discovery Studio Visualizer version 16.1.0. This involved removing existing ligands, adding polar hydrogens, and saving the structures in PDB format. The structures of the compounds were drawn in ChemSketch and saved as .mol files, which were then converted to .pdbqt format in PyRx using Open Babel. We defined a grid around the target protein with dimensions 60 × 60 × 60 Å along X, Y, and Z axes, and with a spacing of 1.5 Å between grid points. Docking was then carried out using this search space. The resulting interactions were visualized in Biovia Discovery Studio, with the interactions saved in 2D format and binding energies recorded in CSV format in an Excel sheet.

FMO studies

The Highest Occupied Molecular Orbital (HOMO) and Lowest Unoccupied Molecular Orbital (LUMO) energies of the target molecule were calculated using ORCA quantum chemistry software (version 5.0) with input parameters generated by Avogadro. The molecules were constructed and optimized in Avogadro to achieve a low-energy conformation. The optimized structures were saved in coordinate (.xyz) format and then converted into an ORCA input file (.inp) using Avogadro's ORCA extension. The calculations were performed using a Restricted Hartree-Fock (RHF) method with geometry optimization and the def2-SVP basis set. Upon execution in ORCA, the HOMO and LUMO energies were obtained from the orbital energy listings in the output's "MOLECULAR ORBITALS" section. The HOMO-LUMO gap was determined by subtracting the HOMO energy from the LUMO energy. This energy gap provides valuable insight into the electronic properties of the molecule, offering indications of its stability and reactivity.

Biological evaluation

The synthesized compounds were screened for antibacterial and antifungal activities. For antibacterial activity against two gram-positive and two gram-negative organisms like *Staphylococcus aureus*, *Enterococcus faecalis*, *Escherichia coli*, and *Klebsiella pneumoniae*. For antifungal activity against *Candida albicans* and *Aspergillus niger* by the cup plate method using nutrient agar medium. Dimethyl formamide (DMF) was used as a solvent control. Ciprofloxacin and fluconazole were used as standards for antibacterial and antifungal screening.

Results

In this study, a series of pyrazole derivatives were successfully synthesized and evaluated through various in silico and in vitro methods. The drug-likeness of the synthesized compounds was assessed using Lipinski's Rule of Five given in Table 2. All compounds exhibited molecular weights under 500 Daltons. LogP values remained below the threshold of 5, indicating favorable lipophilicity. Each compound had one hydrogen bond donor and fewer than 10 hydrogen bond acceptors, reflecting good oral bioavailability potential.

Table 2. Lipinski rule showing molecular properties

CODE	MW	Log P	HBD	HBA
B1	298.81	3.34	1	1
B2	301.73	2.20	1	3
B3	270.76	2.86	1	1
B4	301.73	2.24	1	3
B5	291.18	2.85	1	1
B6	316.78	3.26	1	3
B7	346.81	3.24	1	4
B8	256.73	2.62	1	1
B9	291.18	2.91	1	1

MW: Molecular weight (not > 500 daltons); HBD: Hydrogen bond donor (not >5 HBD); HBA: Hydrogen bond acceptor (not > 10 HBA); LOG P: Lipophilicity (not > 5)

ADMET analysis given in Table 3 revealed high intestinal absorption (>90%) across all compounds, over fluconazole and comparable to ciprofloxacin. The compounds showed varied blood-brain barrier (BBB) permeability, with several demonstrating better or similar log BB values than ciprofloxacin (–0.581) and fluconazole (–1.075). Most compounds didn't inhibit CYP2D6 or CYP3A4 enzymes, with the exception of B1, which is a potential CYP450 inhibitor. None of the compounds were identified as OCT2 substrates. AMES toxicity was detected in B1, B2, and B4, whereas others showed no mutagenicity. Hepatotoxicity was absent in B2 and B4 but present in the remaining derivatives.

Table 3. The results of the ADMET analysis of the synthesized compounds from pKCSM website

Compound code	Absorption	Distribution		Metabolism				Excretion	Toxicity	
	Intestinal absorption (human)	Blood Brain Barrier Permeability		CYP 2D6 substrate	CYP 3A4 substrate	CYP 2D6 Inhibitor	CYP 3A4 Inhibitor	Renal OCT2 substrate	AMES toxicity	Hepatotoxicity
	Numeric (% Absorbed)	Numeric (log BB)	Numeric (log PS)	Categorical (Yes/No)				Categorical (Yes/ No)	Categorical (Yes/No)	
B1	91.647	0.496	-1.043	No	Yes	Yes	Yes	No	Yes	Yes
B2	93.547	-0.231	-1.783	No	Yes	No	No	No	Yes	No
B3	94.795	0.332	-1.305	No	No	No	No	No	No	Yes
B4	93.547	-0.231	-1.783	No	Yes	No	No	No	Yes	No
B5	93.336	0.283	-1.305	No	No	No	No	No	No	Yes
B6	94.99	0.195	-1.443	No	Yes	No	No	No	No	Yes
B7	94.987	0.067	-2.087	No	Yes	No	No	No	No	Yes
B8	94.997	0.341	-1.319	No	No	No	No	No	No	Yes
B9	93.336	0.283	-1.305	No	No	No	No	No	No	Yes
Ciprofloxacin	95.741	-0.581	-2.618	No	Yes	No	No	No	Yes	Yes
fluconazole	85.475	-1.075	-3.405	No	No	No	No	No	Yes	Yes

Several molecular descriptors were computed in Table 4, including GETO, BCUT, QNmin, SITO, Chi10, and the number of rotatable bonds (nrot). The electronic descriptors, particularly GETO and BCUT, showed that compounds B3, B5, and B9 closely resembled ciprofloxacin in terms of electronic distribution. QNmin values were consistent across the series, suggesting a stable charge distribution beneficial for target interactions. Steric descriptors, such as SITO and Chi10, indicated that B3 and B5 had similar spatial arrangements and bulk to ciprofloxacin. B6 and B7 displayed higher Chi10 values, indicating greater branching and structural complexity. Molecular flexibility analysis through NROT revealed that B3 and B8 were relatively rigid, while B7 was more flexible, a trait that can enhance membrane permeability.

Table 4. Molecular descriptors of the synthesized compounds

Compound code	Geto	BCUT				QNmin	Sito	Chi10	NROT
		V2	V3	M12	M16				
B1	2.074	3.797	3.453	1.484	1.082	-0.302	21.355	0.851	3
B2	2.074	3.781	3.399	1.254	0.777	-0.302	15.315	0.797	3
B3	2.113	3.786	3.411	1.356	0.787	-0.302	20.257	0.697	2
B4	2.074	3.781	3.404	1.255	0.779	-0.302	25.45	0.851	3
B5	2.113	3.774	3.39	1.249	0.776	-0.302	20.005	0.684	2
B6	2.07	3.78	3.395	1.431	1.007	-0.302	24.128	0.85	4
B7	2.04	3.785	3.405	1.437	1.082	-0.302	26.207	0.938	5
B8	2.154	3.768	3.386	1.253	0.777	-0.302	19.969	0.64	2
B9	2.113	3.774	3.392	1.238	0.752	-0.302	20.005	0.697	2
Ciprofloxacin	2.11	3.634	3.529	1.372	0.99	-0.367	17.918	1.083	3
Fluconazole	2.059	3.583	3.515	1.309	0.84	-0.25	15.89	0.538	5

Geto: Electronic descriptor, BCUT: Structural descriptors, QNmin: Charge descriptor, Sito: Topological descriptor, Chi10 (Kier's Chi connectivity index): connectivity descriptor, nrot (Number of Rotatable bonds): Flexibility descriptor.

Docking studies were performed against DNA gyrase and 14-alpha demethylase (Table 5). Compounds B3, B5, and B8 showed superior binding affinities to DNA gyrase compared to ciprofloxacin, suggesting strong antibacterial potential. Meanwhile, B1 and B8 exhibited higher binding scores with 14-alpha demethylase than fluconazole, indicating promising antifungal activity.

Table 5. Binding energies of investigational selected ligands with appropriate proteins

Sl. No.	Compound code	Docking score Binding affinity (Kcal/mol)			
		Antibacterial		Antifungal	
		DNA gyrase PDB ID: 6kzx	H-bond	14 alpha demethylase PDB ID: 7RTQ	H-bond
1	B1	-7.9	ASP 73	-8.7	SER 215
2	B2	-8.0	ASP 73, ALA 47, VAL 167	-8.5	SER 215
3	B3	-8.4	ASN 46	-8.6	Hydrophobic
4	B4	-8.2	ARG 76	-8.3	ILE 359, MET 360
5	B5	-8.8	ASP 73	-8.5	GLU 165
6	B6	-7.9	Hydrophobic	-8.4	GLU 165
7	B7	-7.1	ASN 46	-8.2	Hydrophobic
8	B8	-8.5	ASP 73	-8.7	GLU 165
9	B9	-8.1	ASP 73	-8.5	Hydrophobic
10	Standard	-7.4 (Ciprofloxacin)	GLU 50, GLY 77	-7.5 (Fluconazole)	LEU 221, PHE 216

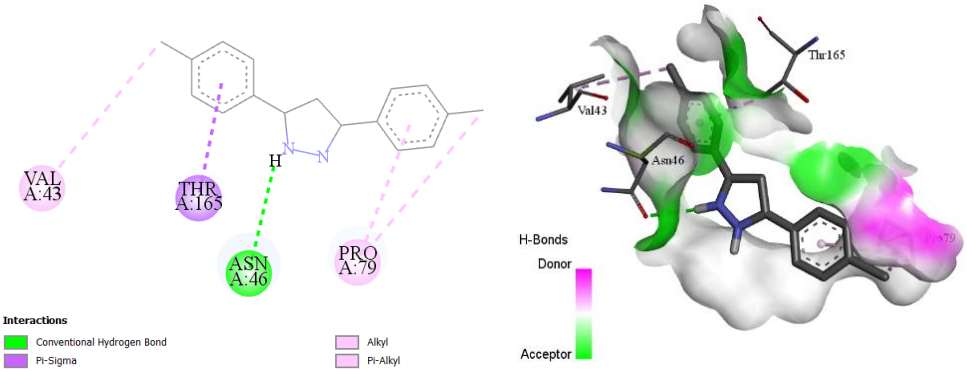

Figure 3. 2D, 3D and hydrogen bond interaction diagram of B5 with anti-bacterial protein (PDB ID: 6KZX)

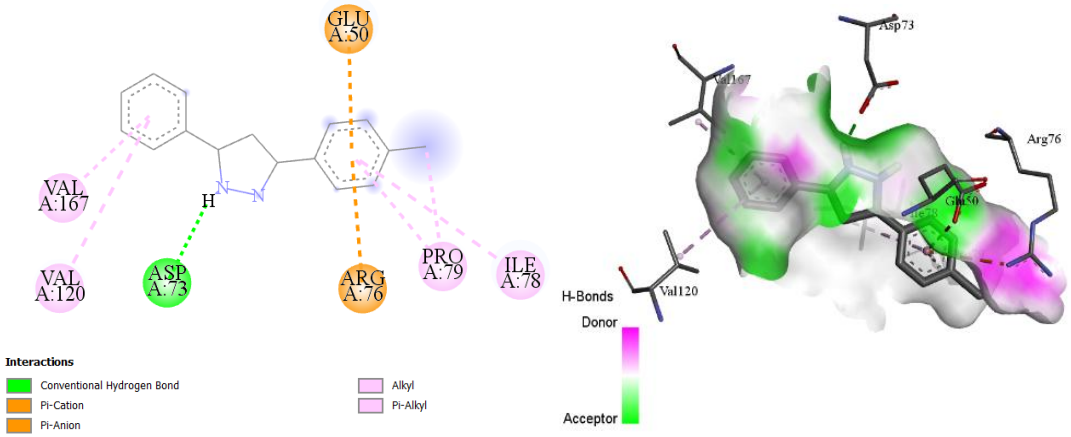

Figure 4. 2D, 3D and hydrogen bond interaction diagram of B8 with anti-bacterial protein (PDB ID: 6KZX)

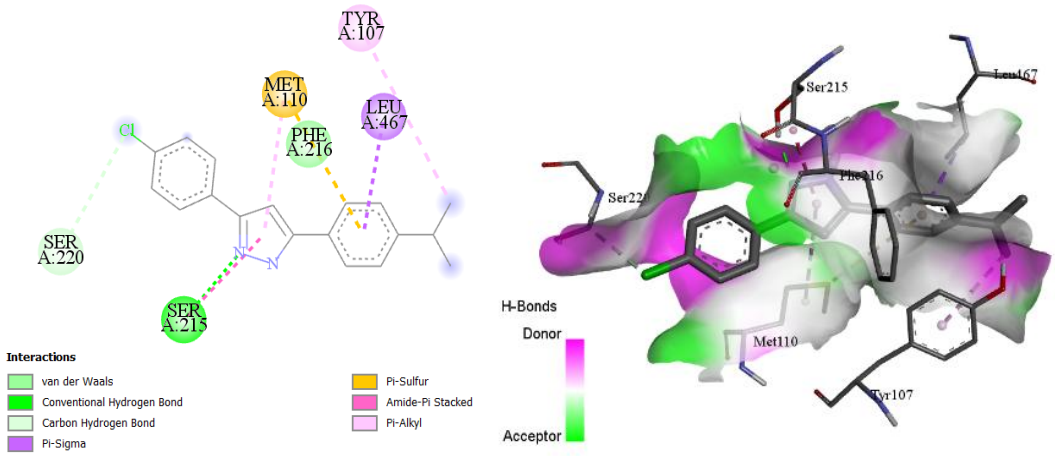

Figure 5. 2D, 3D and hydrogen bond interaction diagram of B1 with anti-fungal protein (PDB ID: 7RTQ)

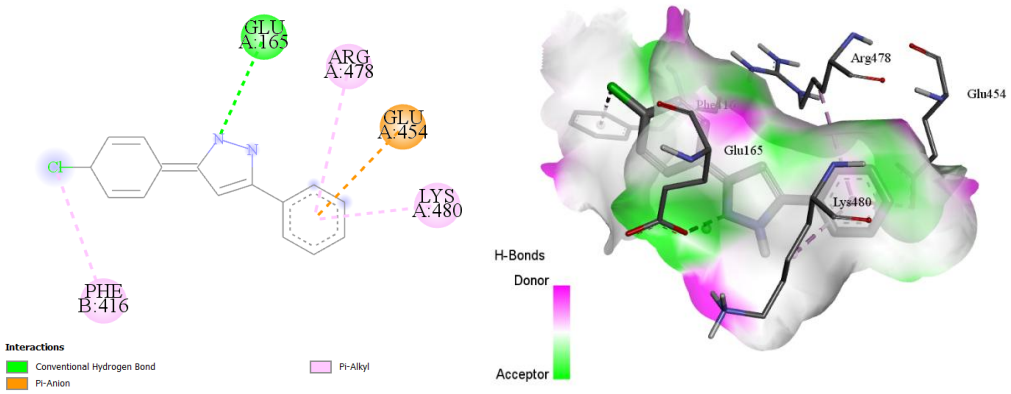

Figure 6. 2D, 3D and hydrogen bond interaction diagram of B8 with anti-fungal protein (PDB ID: 7RTQ)

Total SCF energy and dipole moment of the compounds were calculated and are represented in table 6. Compounds with B5 and B9 showing the most negative total SCF energy. The virial ratio of all compounds is close to 2, as expected for stable systems.

Table 6. Total SCF energy and dipole moment of the synthesized compounds calculated using ORCA software

Compound name	Total SCF energy				Dipole moment				
	Total energy (eV)	**Virial components**			**Total dipole moment**			**Magnitude**	
		Potential Energy (eV)	**Kinetic Energy (eV)**	**Virial ratio**	X	Y	Z	a.u.	Debye
B1	-34294.683	-68468.432	34173.748	2.003	0.97806	0.66622	-0.65929	1.35466	3.44327
B2	-36642.021	-73169.875	36527.854	2.003	-1.76115	0.56045	1.78537	2.56969	6.53163
B3	-32172.069	-64239.568	32067.498	2.003	-1.25990	-0.16731	-0.43010	1.34177	3.41050
B4	-36642.214	-73170.807	36528.592	2.003	0.31703	-0.50049	1.42135	1.53988	3.91406
B5	-43594.307	-87091.828	43497.521	2.002	-0.44260	0.12997	-0.16374	0.48949	1.24417
B6	-37302.847	-74481.100	37178.252	2.003	-2.13702	1.08681	-0.58621	2.46813	6.27348
B7	-40399.115	-80660.881	40261.766	2.003	0.90071	-0.56902	0.78122	1.32112	3.35802
B8	-31110.608	-62124.078	31013.469	2.003	-1.18489	-0.17996	-0.15207	1.20809	3.07072
B9	-43594.304	-87091.927	43497.622	2.002	-0.58993	-0.30892	0.40881	0.78139	1.98615
ciprofloxacin	-31038.928	-61924.489	30885.560	2.004	-2.57723	-1.74240	2.37988	3.91688	9.95591
Fluconazole	-29898.928	-59663.883	29764.955	2.004	-0.89060	-1.83684	0.71716	2.16367	5.49962

Table 7. SCF energy of reactants

SCF energy of Chalcones (C) (eV)	SCF energy of hydrazine hydrate (H) (eV)	SCF energy of reactant (SR)= (C+H) (eV)
-33338.38284 (A1)	-5089.60059	-38427.98343
-35685.73994 (A2)	-5089.60059	-40775.34053
-31215.72880 (A3)	-5089.60059	-36305.32939
-35685.77210 (A4)	-5089.60059	-40775.37269

-42637.91217 (A5)	-5089.60059	-47727.51276
-36346.59665 (A6)	-5089.60059	-41436.19724
-39442.89381 (A7)	-5089.60059	-44532.4944
-30154.19697 (A8)	-5089.60059	-35243.79756
-42637.92533 (A9)	-5089.60059	-47727.52592

The SCF energies of products and reactants are given in Table 7. The reaction energy was calculated by calculating the difference between the SCF energies of products and reactants and is represented in Table 8. The compounds show positive reaction energy around 4133 (eV).

Table 8. Reaction energy required for the formation of product

Compound code	SCF energy of product (SP) (eV)	SCF energy of reactant (SR) (eV)	Reaction energy (SP-SR) (eV)
B1	-34294.683	-38427.98343	4133.30043
B2	-36642.021	-40775.34053	4133.31953
B3	-32172.069	-36305.32939	4133.26039
B4	-36642.214	-40775.37269	4133.15869
B5	-43594.307	-47727.51276	4133.20576
B6	-37302.847	-41436.19724	4133.35024
B7	-40399.115	-44532.4944	4133.3794
B8	-31110.608	-35243.79756	4133.18956
B9	-43594.304	-47727.52592	4133.22192

Table 9. Frontier molecular orbitals of the synthesized and standard compounds

Compound code	Homo	Lumo
B1	-8.292	2.477
B2	-8.459	1.316
B3	-8.839	2.476
B4	-8.643	1.394
B5	-8.448	2.352
B6	-7.976	2.642
B7	-8.317	2.468
B8	-8.330	2.449
B9	-8.447	2.349
Ciprofloxacin	-8.841	1.857

The HOMO-LUMO gaps of the synthesized compounds are similar to the values of Ciprofloxacin (10.97 eV) and Fluconazole (12.31 eV). The electronegativity values of the synthesized compounds (2.67 to 3.57) were also in alignment with ciprofloxacin and fluconazole, 3.49 and 3.85, respectively and the values are given in Table 9. Global chemical reactivity indices like Electron Affinity, Electronegativity, Electrochemical Potential etc. are given in Table 10.

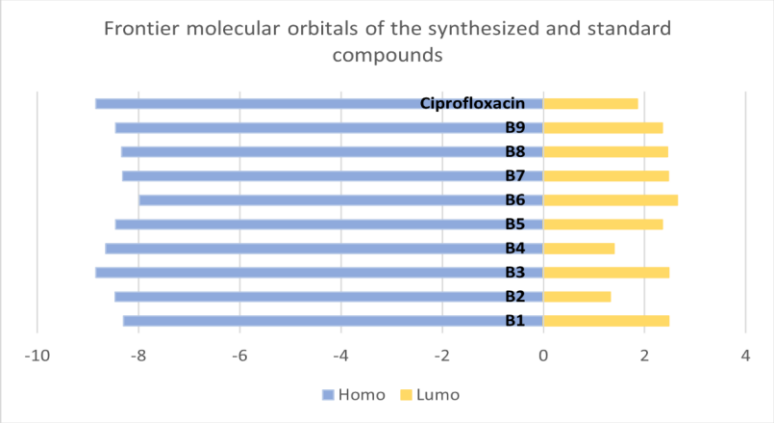

Figure 7. Graph representing the Frontier molecular orbitals of the synthesized and standard compounds

Table 10. Global chemical reactivity indices for synthesized (B1-B9) and standard compounds

Compound code	Homo Lumo gap (ΔE)	Electron affinity (A)	Ionization potential (I)	Electro-negativity (χ)	Chemical hardness (η)	Chemical softness (s)	Electrochemical potential (μ)	Electrophilicity index (ω)
B1	10.769	-2.477	8.292	2.9075	5.3845	0.185718	-5.3845	2.69217
B2	9.775	-1.316	8.459	3.5715	4.8875	0.204603	-4.8875	2.44375
B3	11.315	-2.476	8.839	3.1815	5.6575	0.176756	-5.6575	2.82875
B4	10.037	-1.394	8.643	3.6245	5.0185	0.199262	-5.0185	2.50925
B5	10.8	-2.352	8.448	3.048	5.416	0.18463	-5.4	2.69202
B6	10.618	-2.642	7.976	2.667	5.309	0.188359	-5.309	2.6545
B7	10.785	-2.468	8.317	2.9245	5.3925	0.185442	-5.3925	2.69625
B8	10.779	-2.449	8.330	2.9405	5.3895	0.185545	-5.3895	2.69475
B9	10.796	-2.349	8.447	3.049	5.398	0.185253	-5.398	2.699
Ciprofloxacin	10.968	-1.857	8.841	3.492	5.349	0.186950	-5.484	2.81120
Fluconazole	12.312	-2.304	10.008	3.852	6.156	0.162443	-6.516	3.44852

Gap: **ΔE**= $E_{LUMO}-E_{HOMO}$, **Electron Affinity**: **A**= $-E_{LUMO}$, **Ionization Potential**: **I**= $-E_{HOMO}$, **Electronegativity**: **χ**= (I+A)/2, **Chemical Hardness**: **η**= (I−A)/2, **Chemical Softness**: **S**= 1/η, **Electronic Chemical Potential**: **μ**= −I+A/2, **Electrophilicity Index**: **ω**= $\mu^2/2\eta$

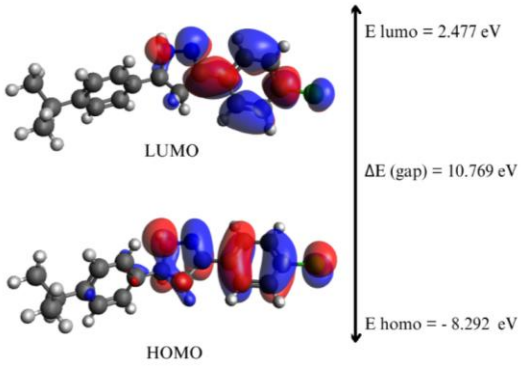

Figure 8. Illustration of HOMO LUMO and energy gap of the compound B1

The antibacterial and antifungal activities were performed using the cup plate method, and the results are given in the tables 11 & 12. All the synthesized compounds showed good to moderate activity.

Table 11. Anti-bacterial evaluation for synthesized compounds using cup plate method

Compound code	**Zone of inhibition (mm)** (SD ± 0.5)							
	Staphylococcus aureus		***Escherichia coli***		***Klebsiella pneumoniae***		***Enterococcus faecalis***	
	200 μg/ml	**400 μg/ml**	**200 μg/ml**	**400 μg/ml**	**200 μg/ml**	**400 μg/ml**	**200 μg/ml**	**400 μg/ml**
B1	-	12	20	26	-	23	-	18
B2	-	13	19	25	-	22	-	16
B3	-	12	21	27	-	22	-	14
B4	-	14	19	26	-	24	-	15
B5	-	15	20	25	-	23	-	17
B6	-	14	19	27	-	25	-	18
B7	-	14	20	22	-	24	-	16
B8	-	14	18	25	-	21	-	17
B9	-	13	21	26	-	23	-	18
Standard 400 μg/ml Ciprofloxacin	41		25		41		40	
Control	-		-		-		-	

'-' indicates that bacterial growth was not inhibited

Table 12. Anti-fungal evaluation for synthesized compounds using cup plate method

Compound code	Zone of inhibition (mm) (SD is ± 0.5)			
	Candida albicans		*Aspergillus niger*	
	200 µg/ml	400 µg/ml	200 µg/ml	400 µg/ml
B1	15	17	16	23
B2	12	16	15	20
B3	10	15	17	21
B4	12	16	13	19
B5	11	17	19	23
B6	15	20	16	21
B7	14	20	11	19
B8	13	16	15	22
B9	12	15	12	17
Standard 400 µg/ml Fluconazole	25		40	
Control	-		-	

'-' indicates that fungal growth was not inhibited

Discussion

The use of an ultrasonicator for synthesizing pyrazoles resulted in high yields and reduced reaction time to 15-20 mins; in previous studies it is shown to take up to 8 hours (Loh et al., 2013). The substituted pyrazoles were then recrystallized using ethanol to get pure compounds. The synthesized compounds were confirmed by TLC (pet ether:ethyl acetate 8:2), melting point, FTIR, and ^{1}H-NMR spectroscopy. In FTIR spectroscopy, a single band at 3350-3310 cm^{-1} for -NH stretching indicates the formation of a secondary amine, and C=N was observable at 1500 cm^{-1}. In ^{1}H-NMR spectroscopy, the ABX splitting pattern was observable (Singh et al., 2010); the individual protons of The -$CH_{2\,(a,b)}$ and -CH (x) proton peaks of the pyrazole ring are observed as H_a, H_b, and H_x as individual multiplets and are observed at δ 2-5 ppm. The aromatic protons are observed at 7-9 ppm. The synthesized pyrazole derivatives were evaluated based on Lipinski's Rule of Five. They possess favorable drug-like properties with potential for good oral bioavailability (Caminero et al., 2023). The ADMET analysis reveals high intestinal absorption across all compounds, indicating effective oral bioavailability similar to ciprofloxacin and better than fluconazole. The blood-brain barrier permeability varies among compounds, with some potentially showing better or comparable BBB penetration relative to standard drugs. Most of the synthesized compounds didn't inhibit CYP2D6 or CYP3A4, except for one compound suggesting Cytochrome P450 inhibition. None are substrates for renal OCT2, indicating a lower likelihood of affecting renal excretion. Several compounds show AMES toxicity, suggesting potential mutagenicity. This is consistent with findings for ciprofloxacin and fluconazole. Hepatotoxicity is also observed in some synthesized compounds, indicating the need for further evaluation regarding mutagenicity and hepatotoxicity. Molecular descriptors, like the electronic parameters such as Geto and BCUT, reveal that compounds B3, B5, and B9 have the possibility of comparable binding interactions at the molecular level with ciprofloxacin, which is promising for their biological activity. Additionally, the QNmin values across these compounds show minimal variance, implying a stable and consistent charge distribution helps in electrostatic interactions within biological systems. The uniformity of QNmin values suggests they may achieve similar stability in target binding as ciprofloxacin and fluconazole. The steric descriptors Sito and Chi10 proved to be particularly informative in understanding the spatial characteristics of the synthesized compounds. Notably, B3 and B5 demonstrated Sito values comparable to ciprofloxacin, suggesting that these compounds may share similar steric requirements for effective accommodation within biological targets of analogous topology. Such similarity could be advantageous in achieving favorable docking orientations and stable ligand–receptor interactions. The Chi10 descriptor, reflecting molecular branching and structural complexity, further highlighted differences across the series. Higher Chi10 values indicate increased molecular complexity, which may enhance stability and reduce susceptibility to enzymatic degradation, thereby contributing to prolonged biological activity and improved pharmacokinetic properties. In addition, molecular flexibility, as assessed through the number of rotatable bonds (nrot), provided crucial insights into conformational adaptability. Compounds such as B3 and B8, with lower nrot values, exhibited greater rigidity, which could favor binding affinity and target specificity by minimizing entropic penalties. By contrast, B7, with a higher nrot value, displayed enhanced conformational flexibility, which may promote absorption and distribution in vivo. Overall, these findings underscore the importance of maintaining a balance between rigidity and flexibility, as both steric and topological features influence binding affinity, stability, and pharmacokinetic behavior. Such balance is essential for optimizing therapeutic performance, aligning with previous reports that highlight the critical role of molecular descriptors in drug design (Dong et al., 2015). Molecular docking was performed to assess

the antibacterial and antifungal potential of the synthesized compounds by targeting DNA gyrase (PDB ID: 6kzx) and 14α-demethylase (PDB ID: 7RTQ), two essential microbial enzymes involved in DNA supercoiling and ergosterol biosynthesis, respectively. For DNA gyrase, compound B5 showed the strongest binding affinity (-8.8 kcal/mol), higher than ciprofloxacin (-7.4 kcal/mol). B5 formed a key hydrogen bond with Asp73, contributing to binding stability. Compounds B8 (-8.5 kcal/mol) and B3 (-8.4 kcal/mol) also interacted with residues Asp73, Asn46, and Arg76 through hydrogen bonding and hydrophobic contacts. In contrast, ciprofloxacin showed fewer interactions and weaker binding. These findings highlight the superior binding potential of the synthesized derivatives compared to the standard drug. Against 14α-demethylase, compounds B1 and B8 exhibited the best affinities (-8.7 kcal/mol), outperforming fluconazole (-7.5 kcal/mol). Both formed hydrogen bonds with Glu165 and Ser215 at the active site. Other compounds such as B3 (-8.6 kcal/mol) displayed strong hydrophobic interactions with residues like Ile359 and Met360, indicating that both hydrogen bonding and hydrophobic contacts contribute to enhanced binding. Overall, the docking results support the promising anti-bacterial potential of these compounds. Across both targets, the presence of a pyrazole moiety with accessible -NH groups was found to be crucial for hydrogen bonding, especially in compounds like B1, B5, and B8. This functional group likely increases electron density and polarity, allowing for stronger and more directed interactions with the protein's polar residues. Additionally, non-H-bonding interactions such as van der Waals forces and hydrophobic packing were also found to significantly contribute to the overall stability and affinity of the ligand-protein complexes. The total SCF energy (eV) is a key indicator of the overall stability of the compounds. Lower total SCF energies generally indicate more stable compounds. Compounds with B5 and B9, indicating potentially greater stability along with other compounds at a similar range. The virial ratio of all compounds is close to 2, as expected for stable systems. The reaction energy was calculated by calculating the difference between the SCF energies of product and reactant. The compounds show positive reaction energy around 4133 eV; this indicates that the transformations from reactants to products require energy input. The reactions are endothermic, meaning that energy must be supplied for the reaction to proceed. The need for energy input suggests that the reactants are not in an energetically favorable state for the reaction to occur spontaneously. A literature survey has shown that the reaction time using conventional heating methods requires more than 8 hours (Loh et al., 2013). Therefore, in this research, we use an ultrasonicator to reduce the reaction time. ultrasound (which provides localized high-energy environments) especially useful to overcome the energy barrier and drive the reactions to completion. The cavitation effect generated by ultrasound provides the necessary energy to help the compounds reach their transition state, despite the overall positive reaction energy. The uniformity of the reaction energy values (all around 4133 eV) across different compounds suggests that these compounds undergo similar transformations, requiring approximately the same amount of energy to proceed. This is the result of a common reaction mechanism or similar types of molecular interactions during the transformation process. The frontier orbital analysis of the synthesized derivatives and the standard compound Ciprofloxacin shows that the HOMO–LUMO energy gaps are closely matched, reflecting comparable electronic stability and reactivity (Table 9). The HOMO values range from –8.84 to –7.98 eV while the LUMO values span +1.32 to +2.64 eV; the resulting gaps cluster around ~10–11 eV, very similar to Ciprofloxacin's 10.97 eV. The calculated electronegativity values (2.67–3.57) likewise fall within the narrow window defined by Ciprofloxacin (3.49) and Fluconazole (3.85). This alignment indicates that the novel derivatives potentially mimic the electronic profile of the standards, supporting their plausible biological activity. By presenting this data graphically (Fig 7), readers can quickly appreciate the uniformity of electronic behavior across the series and contextualize it against the benchmark compounds. These similarities suggest that the synthesized compounds share similar reactivity profiles with the standards (Khan et al., 2024). A higher electronegativity allows the compound to interact more effectively with electron-rich regions in bacterial and fungal cells, which often contain nucleophilic sites, such as those on DNA or enzymes. This electron-rich interaction plays a key role in inhibiting microbial growth and proliferation, correlating with the antibacterial and antifungal activities. Chemical hardness measures a molecule's resistance to changes in electron density. Higher hardness values indicate a stable, less reactive compound, as it is less likely to gain or lose electrons. Softness, the inverse of hardness, measures a molecule's tendency to undergo electronic changes. Softer compounds are more reactive and readily interact with other biological macromolecules, especially in reactions where electron transfer is involved. Synthesized compounds showed similar amount of hardness and softness when compared with ciprofloxacin. The electrochemical potential and electrophilicity index are also important in assessing the molecule's ability to participate in electron-transfer reactions, which are important for the anti-bacterial activity. Compounds with a lower electrochemical potential and higher electrophilicity index are expected to exhibit strong electrophilic character, facilitating their ability to react with nucleophilic components in bacterial and fungal cells. The synthesized compounds have showed the similar pattern and are similar to that of standard ciprofloxacin. The comparable electrochemical parameters suggest that these compounds may share a similarity to interact with microbial cells and potentially disrupt essential cellular processes, underscoring their promising potential as anti-bacterial agents.

Among the tested bacteria, *Escherichia coli* showed the highest sensitivity to the synthesized compounds. Compounds B5 and B6 demonstrated consistent antibacterial activity against both Gram-positive and Gram-negative strains, though their potency was lower compared to ciprofloxacin. Antifungal screening by the cup plate method revealed moderate

activity of the compounds. B1 and B5 showed notable inhibition (23 mm) against *Aspergillus niger*, while B6 and B7 were more effective against *Candida albicans*, which was supported by favorable docking scores (-8.4 and -8.2 kcal/mol, respectively). Nevertheless, their activity remained inferior to fluconazole, particularly against *A. niger*, though against *C. albicans* they exhibited consistent but lower potency.

Conclusion

Given the rising issue of anti-bacterial resistance, the development of effective anti-bacterial agents is critical along with the sustainable method. Our research contributes to this effort by offering pyrazole derivatives with potential as therapeutic agents using an energy-efficient method, i.e., ultrasonication. In this study, pyrazole derivatives were successfully synthesized using ultrasound-assisted methods, a green chemistry approach that improves reaction efficiency while minimizing environmental impact. Notably, the reaction times were shortened to just 15–20 minutes, representing a significant breakthrough. Various in silico studies were performed like lipinski's rule of 5 studies, ADMET studies, molecular descriptor studies, molecular docking, and FMO (HOMO-LUMO) studies. The results of in silico studies were compared with the standards ciprofloxacin and fluconazole. Results indicated that synthesized compounds have similar properties to those of standards. Finally, in vitro studies were conducted for antibacterial and antifungal activities. Compounds have shown good antibacterial and antifungal activity collectively. However, the synthesized compounds were less potent in comparison with standard compounds. Further modification in the structure will help in obtaining highly active compounds.

Acknowledgement

None.

Author contributions

All authors have contributed equally in this current work.

Conflict of interests

The authors declare no conflict of interest.

Funding

No funding has been made from anyone for this current work.

Ethics approval

Not applicable.

AI Usage Declaration

During the preparation of this manuscript, the authors used language-enhancement tools such as QuillBot and ChatGPT strictly for improving phrasing, grammar, and overall readability. All content generated by these tools was thoroughly reviewed and edited by the authors, who take full responsibility for the final text.

References

Ivanković, A., Dronjić, A., Bevanda, A. M., & Talić, S. (2017). Review of 12 principles of green chemistry in practice. *International Journal of Sustainable and Green Energy, 6*(3), 39-48.

Anastas, P. T., Kirchhoff, M. M., & Williamson, T. C. (2001). Catalysis as a foundational pillar of green chemistry. *Applied Catalysis A: General, 221*(1-2), 3-13.

Banerjee, B. (2017). Recent developments on ultrasound assisted catalyst-free organic synthesis. *Ultrasonics Sonochemistry, 35*, 1–4.

Rudrapal, M., Khan, J., Dukhyil, A. A., Alarousy, R. M., Attah, E. I., Sharma, T., Khairnar, S. J., & Bendale, A. R. (2021). Chalcone scaffolds, bioprecursors of flavonoids: Chemistry, bioactivities, and pharmacokinetics. *Molecules, 26*(23), 7177.

Mahmood, S., Khan, S. G., Rasul, A., Christensen, J. B., & Abourehab, M. A. S. (2022). Ultrasound Assisted Synthesis and In Silico Modelling of 1,2,4-Triazole Coupled Acetamide Derivatives of 2-(4-Isobutyl phenyl) propanoic acid as Potential Anticancer Agents. *Molecules, 27*(22), 7984.

Bukhari, S. N. A., Jasamai, M., & Jantan, I. (2012). Synthesis and biological evaluation of chalcone derivatives (mini review). *Mini-Reviews in Medicinal Chemistry, 12*(13), 1394–1403.

Teli, G., & Chawla, P. A. (2021). Hybridization of imidazole with various heterocycles in targeting cancer: A decade's work. *ChemistrySelect, 6*(19), 4803–4836.

Jaiswal, S. (2019). Five and six membered heterocyclic compound with anti-bacterial activity. *Journal of Modern Trends in Science and Technology, 5*, 36–39

Prasad, Y. R., Raja Sekhar, K. K., Shankarananth, V., Sireesha, G., Swetha Harika, K., & Poroikov, V. (2011). Synthesis and in silico biological activity evaluation of some 1,3,5-trisubstituted-2-pyrazolines. *Journal of Pharmacy Research, 4*(2), 558–560

Karrouchi, K., Radi, S., Ramli, Y., Taoufik, J., Mabkhot, Y. N., Al-Aizari, F. A., & Ansar, M. H. (2018). Synthesis and pharmacological activities of pyrazole derivatives: A review. *Molecules, 23*(1), 134.

Bécerra, D., & Castillo, J.-C. (2025). Recent advances in the synthesis of anticancer pyrazole derivatives using microwave, ultrasound, and mechanochemical techniques. RSC Advances. https://doi.org/10.1039/D4RA08866B

Sharif, M. S., Aqeel, M., Haider, A., Naz, S., Ikram, M., Ul-Hamid, A., Haider, J., Aslam, I., Nazir, A., & Butt, A. R. (2021). Photocatalytic, bactericidal and molecular docking analysis of annealed tin oxide nanostructures. *Nanoscale Research Letters, 16*, 1–6.

Rathee, A., Solanki, P., Emad, N. A., Zai, I., Ahmad, S., Alam, S., Alqahtani, A. S., Noman, O. M., Kohli, K., & Sultana, Y. (2024). Posaconazole-hemp seed oil loaded nanomicelles for invasive fungal disease. *Scientific Reports, 14*(1), 16588.

Loh, W. S., Quah, C. K., Chia, T. S., Fun, H. K., Sapnakumari, M., Narayana, B., & Sarojini, B. K. (2013). Synthesis and crystal structures of N-substituted pyrazolines. *Molecules (Basel, Switzerland), 18*(2), 2386–2396.

Singh, P., Jagmohan, S., Negi, G., Pant, J. N., & Rawat, M. S. M. (2010). 5-(3-Nitrophenyl)-3-phenyl-4,5-dihydro-1H-pyrazole-1-carbaldehyde. *Molbank, 2010*(1), M650.

Caminero Gomes Soares, A., Marques Sousa, G. H., Calil, R. L., & Goulart Trossini, G. H. (2023). Absorption matters: A closer look at popular oral bioavailability rules for drug approvals. *Molecular informatics, 42*(11), e202300115.

Dong, J., Cao, D. S., Miao, H. Y., Liu, S., Deng, B. C., Yun, Y. H., Wang, N. N., Lu, A. P., Zeng, W. B., & Chen, A. F. (2015). ChemDes: an integrated web-based platform for molecular descriptor and fingerprint computation. *Journal of cheminformatics, 7*, 60.

Khan, M. A., Mutahir, S., Tariq, M. A., & Almehizia, A. A. (2024). Exploration of Specific Fluoroquinolone Interaction with SARS-CoV-2 Main Protease (Mpro) to Battle COVID-19: DFT, Molecular Docking, ADME and Cardiotoxicity Studies. *Molecules (Basel, Switzerland), 29*(19), 4721.